

# Balancing Water Dissociation and Current Densities To Enable Sustainable Hydrogen Production with Bipolar Membranes in Microbial Electrolysis Cells

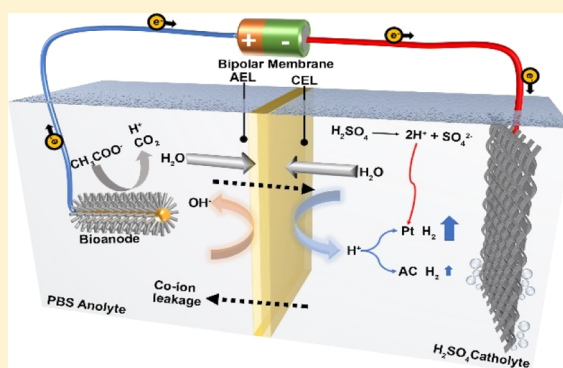
Xu Wang,<sup>\*,†,‡</sup> Ruggero Rossi,<sup>‡</sup> Zhifei Yan,<sup>§</sup> Wulin Yang,<sup>‡</sup> Michael A. Hickner,<sup>§,||</sup> Thomas E. Mallouk,<sup>§</sup> and Bruce E. Logan<sup>\*,‡,Ⓜ</sup>

<sup>†</sup>School of Resource and Environmental Sciences, Hubei International Scientific and Technological Cooperation Base of Sustainable Resource and Energy, Wuhan University, No. 129 Luoyu Road, Wuhan 430079, P. R. China

<sup>‡</sup>Department of Civil and Environmental Engineering, <sup>§</sup>Department of Chemistry, and <sup>||</sup>Department of Materials Science and Engineering, The Pennsylvania State University, University Park, State College, Pennsylvania 16802, United States

## Supporting Information

**ABSTRACT:** Hydrogen production using two-chamber microbial electrolysis cells (MECs) is usually adversely impacted by a rapid rise in catholyte pH because of proton consumption for the hydrogen evolution reaction. While using a bipolar membrane (BPM) will maintain a more constant electrolyte pH, the large voltage loss across this membrane reduces performance. To overcome these limitations, we used an acidic catholyte to compensate for the potential loss incurred by using a BPM. A hydrogen production rate of  $1.2 \pm 0.7$  L- $H_2$ /L/d ( $j_{\max} = 10 \pm 0.4$  A/m<sup>2</sup>) was obtained using a Pt cathode and BPM with a pH difference ( $\Delta$ pH = 6.1) between the two chambers. This production rate was 2.8 times greater than that of a conventional MEC with an anion exchange membrane (AEM,  $0.43 \pm 0.1$  L- $H_2$ /L/d,  $j_{\max} = 6.5 \pm 0.3$  A/m<sup>2</sup>). The catholyte pH gradually increased to  $11 \pm 0.3$  over 9 days using the BPM and Pt/C, which decreased current production ( $j_{\max} = 2.5 \pm 0.3$  A/m<sup>2</sup>). However, this performance was much better than that obtained using an AEM as the catholyte pH increased to  $10 \pm 0.4$  after just one day. The use of an activated carbon cathode with the BPM enabled stable performance over a longer period of 12 days, although it reduced the hydrogen production rate ( $0.45 \pm 0.1$  L- $H_2$ /L/d).



## INTRODUCTION

Microbial electrolysis cells (MECs) are electrochemical devices that can be used to remove organic matter from wastewaters while electrochemically producing hydrogen at the cathode, requiring only a small applied voltage to make the reaction thermodynamically favorable ( $>0.13$  V at neutral pH).<sup>1</sup> When organic matter is oxidized by exoelectrogens on the anode, protons are released into the solution which can decrease the local solution pH.<sup>2,3</sup> At the cathode, either protons are consumed (at acidic to neutral pHs) or water dissociation provides a proton for the hydrogen evolution reaction (HER) releasing a hydroxide ion (neutral to alkaline pHs), both of which result in an increase in local pH. In a single-chamber MEC, release of these ions into solution would lead to no net change in the bulk pH. However, release of  $H_2$  gas into the electrolyte in a single chamber MEC can result in the loss of  $H_2$  to methane production, or hydrogen oxidation at the anode by the exoelectrogens (hydrogen cross-over) which results in current generation but no net hydrogen gas production.<sup>4,5</sup> To avoid these  $H_2$  losses, a membrane can be used to form a two-chamber MEC to keep the hydrogen gas contained in the

catholyte allowing the separation of the produced gas from the anolyte.<sup>6</sup>

Anion exchange membranes (AEMs) or cation exchange membranes (CEMs) have been used in MECs to separate the electrolyte into two chambers.<sup>2,7–9</sup> However, adding a membrane produces other undesirable outcomes, including changes in the pH of each electrolyte which adversely impacts electrode performance and loss of voltage because of the additional internal resistance of the membrane. With a CEM and a phosphate buffer solution (PBS) electrolyte, the charge is balanced by more abundant cations than protons, such as  $Na^+$  or  $K^+$ , resulting in the acidification of the anolyte and alkalization of the catholyte.<sup>10,11</sup> A decrease in the anolyte pH to  $<6$  can greatly reduce current generation by exoelectrogens, while a rise in catholyte pH adversely impacts the HER.<sup>12</sup> Current densities produced using an AEM are typically higher than those obtained with a CEM, as the charge can be better

Received: August 21, 2019

Revised: November 9, 2019

Accepted: November 12, 2019

Published: November 12, 2019

balanced by the high concentration of phosphate anions when using a PBS typically at a concentration of 50 mM.<sup>10</sup> In addition, the internal resistance is increased more with a CEM (435 mΩ m<sup>2</sup>, Nafion) than it is with a typical AEM (192 mΩ m<sup>2</sup>, Fumasep FAA).<sup>10</sup> Thus, methods are needed to mitigate or avoid pH changes as well as to improve the performance of MECs.

In this study, we examined the use of a reverse-bias bipolar membrane (BPM) in an MEC to maintain electrolyte pH in order to avoid operation with an unfavorable alkaline catholyte pH (Figure 1). In a reverse-bias configuration, the cation

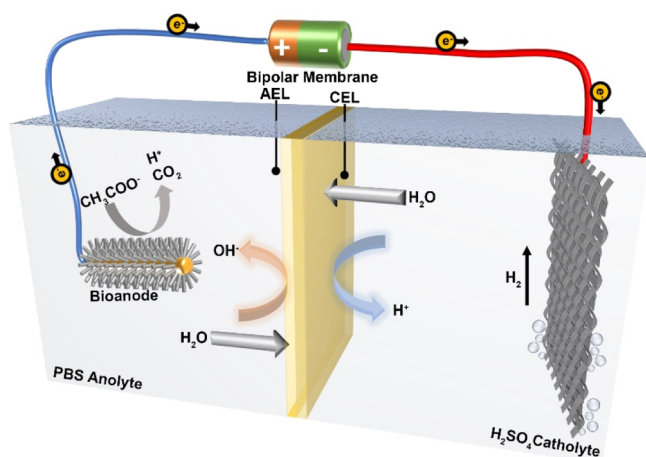


**Figure 1.** Schematic diagram of the BPM-MEC with the H<sub>2</sub>SO<sub>4</sub> catholyte.

exchange layer (CEL) of the BPM faces the cathode and anion exchange layer (AEL) faces the anode. BPMs can be used to minimize the ion cross-over in electrochemical devices and maintain pH differences.<sup>13,14</sup> With current production, water molecules at the junction of the BPM dissociate to hydroxides and protons, balancing the ionic charge in each chamber (Figure 1). However, the process is not perfect as a small amount of ions is able to pass through both ion exchange layers, which is called co-ion leakage.<sup>13,14</sup> A main disadvantage of using a BPM is that a voltage drop is incurred in generating strong acid and base from water at the AEL/CEL interface. This increases the membrane resistance compared to the use of a single AEM or CEM.<sup>15</sup> However, if the cathode and anode are operated in acid and base, respectively, the membrane voltage drop for water dissociation is compensated by the Nernstian shifts in cathode and anode potentials.<sup>16</sup> When an acidic catholyte is used instead of PBS, the potential of the cathode reaction ( $E_{\text{Cat}}$ ) will shift to a more positive potential, for example, from  $-800$  to  $-417$  mV versus Ag/AgCl based on a pH change from 7.5 to 1 using the Nernst equation [ $(7.5 - \text{pH}_{\text{cat}}) \times 59$  mV] (Figure 1). Additionally, the Ohmic loss of a BPM cannot be eliminated and will increase with a higher current density in the device. Previous studies on abiotic electrolysis or photo-electrolysis of water with a BPM and an acidic catholyte were conducted under applied voltages or solar power.<sup>13,16–18</sup> MECs usually operate under lower applied potentials of  $<1.0$  V to obtain high energy recovery and avoid oxygen evolution on the bioanode.<sup>19</sup> A recent study on a coupled microbial photoelectrochemical system using a BPM and acidic catholyte showed that the black silicon (b-Si) photocathode with a “Swiss-cheese” interface was durable in the reactor during a 90 h test and produced 0.8 L H<sub>2</sub> per

catholyte volume per day.<sup>20</sup> Here, we examined the impact of the BPM and acidic catholyte in regular MECs on H<sub>2</sub> production using two different types of cathodes [Pt and activated carbon (AC)], with an MEC containing an AEM as a control. AC is a low cost and abundant material which makes it better suited for wastewater treatment applications than a Pt catalyst. Polarization data were used to quantify the electrode and effective membrane resistances using a recently developed electrode potential slope (EPS) method, as this approach allows for direct comparisons of the components of the resistances under different operational conditions.<sup>21,22</sup> The long-term stability of MECs with BPMs and the acidic catholyte was compared to that of the MECs using an AEM with its catholyte replaced daily. Additionally, a graphene oxide-catalyzed BPM (GO-BPM), which has been reported to catalyze water dissociation in the membrane junction, was also compared to a standard BPM to determine if using this material could reduce internal resistance.<sup>17</sup>

## MATERIALS AND METHODS

**MEC Cathode Preparation.** Two types of cathodes were tested: Pt on carbon cloth (Pt/C) and AC powder (NORIT SX Plus, Norit Americas Inc., TX). Pt/C cathodes were prepared as previously described.<sup>23</sup> Briefly, 35 mg of Pt/C (10 wt %, E-TEK) and 467 μL of Nafion ionomer (5 wt % solution, Dupont, US) were mixed with 233 μL of ethanol by vortexing and brushed onto the carbon cloth [30% poly-(tetrafluoroethylene) (PTFE) treated, Fuel Cell Earth, US; 3 cm in diameter, 7 cm<sup>2</sup> projected area]. The cathodes were then dried overnight in an oven (80 °C). To make the AC cathodes, 2 g of AC powder and 433 μL of PTFE (60 wt % emulsion) were mixed in 75 mL of ethanol using a magnetic stir bar at 60 °C.<sup>24</sup> The gel that formed was cast onto the carbon cloth electrode and cold-pressed together at  $3 \times 10^7$  Pa for 15 s. The electrodes were then dried overnight in an oven (60 °C). The final catalyst loading of Pt/C and AC cathodes was determined by normalizing the weight difference before and after catalyst coating by the projected area of the electrode. Cathodes were glued to a titanium wire using electrically conductive carbon cement (Leit-C, SPI Supplies, Germany) and any exposed wire insulated with epoxy.

**Membranes.** Three different membranes were used: a commercial BPM (FBM, Fumatech, Germany); an AEM (Selemon AMV, AGC Engineering Co. Ltd., Japan); and a thin in-house fabricated BPM containing 4 layers of GO as an interfacial catalyst. To make the GO-BPM, a solvent exchange process was first employed to replace water and alcohol in a Nafion 117 solution (5 wt % in alcohol and water) with *N,N*-dimethylformamide (DMF). The Nafion solution (20 mL) was heated under a vacuum in a water bath at 50 °C to reduce its volume to 10% of the original volume, then 20 mL of DMF was added to the solution, and the mixture was placed under a vacuum oven at 80 °C. This process was repeated five times to ensure complete solvent exchange, producing a final 20 mL solution containing 5% Nafion in DMF (DMF–Nafion). An AEL [brominated polyphenylene oxide (PPO) functionalized with quaternary ammonium groups] was placed onto a glass substrate and held using double-sided tape. The edges of the exposed side of the AEL were covered with Kapton tape to mask a 5 cm × 5 cm area. The GO solution containing 1 g/L of GO single-layer sheets (5–10 μm) in water for fabricating the BPM was prepared in our laboratory using the method of Kovtyukhova et al.<sup>17,25</sup> This GO solution (10 mL) was

dropped onto the exposed AEL surface and left to stand for 20 min.<sup>18,21</sup> After washing thoroughly with nanopure water and then being air dried, 4 mL of the DMF–Nafion solution was air-sprayed onto the GO-modified AEL, and the assembly was heated to 120–130 °C on a hot plate for 1 h to increase the cation conductivity in the Nafion CEL. The BPM was then dried in a convection oven at 60 °C overnight, and stored in 500 mM KNO<sub>3</sub> solution before testing.

**MEC Configuration and Operation.** The MECs were cubic reactors with two chambers each 28 mL in volume (4 cm in length, 3 cm in diameter) separated by a membrane. A glass tube (7.5 cm in length, 1.5 cm in diameter) was mounted on top of the cathode chamber, and sealed with a thick butyl rubber stopper as previously described.<sup>8</sup> Hydrogen gas was collected using gas bags (0.5 L, Calibrated Instruments, US) by inserting two needles connected with a tube through the rubber stoppers of the bag and glass tube. The anode was a graphite brush electrode (2.5 cm in length, 2.5 cm diameter, Mill-Rose, US), with a gap of 1.0 cm between the electrode and membrane. The anode was inoculated, acclimated, and operated in an air cathode microbial fuel cell for more than one year before being used in tests here. In both cases, the same medium was used that contained: sodium acetate in 50 mM PBS (1.5 g/L sodium acetate, 4.58 g/L Na<sub>2</sub>HPO<sub>4</sub>, 2.45 g/L NaH<sub>2</sub>PO<sub>4</sub>·H<sub>2</sub>O, 0.31 g/L NH<sub>4</sub>Cl, 0.13 g/L KCl, 12.5 mL/L trace minerals, and 5 mL/L vitamins). Anodes were transferred to the MECs that were operated with a set applied voltage of 0.9 V (except as noted). The MEC current output was monitored using a multimeter (model 2700, Keithley Instruments Inc., US) by measuring the voltage across a 10 Ω resistor. The catholytes for the BPM–Pt tests contained different concentrations of the H<sub>2</sub>SO<sub>4</sub> catholyte to achieve initial pHs of: 0.3 ± 0.1 (500 mM), 1.4 ± 0.2 (50 mM), 2.2 ± 0.1 (5 mM), and 3.2 ± 0.2 (0.5 mM), except for pH 7.5 ± 0.1 (50 mM PBS). The conductivity of the solution with a pH = 2.2 ± 0.1 was adjusted to 28 ± 0.7 mS/cm, and the pH of the 3.2 ± 0.2 solution was adjusted to 26 ± 0.5 mS/cm using KCl in order to approximately match that of the 50 mM H<sub>2</sub>SO<sub>4</sub> (25 ± 0.5 mS/cm, pH = 1.5). Comparisons of the different membranes and catholytes were made for: BPM–Pt and BPM–AC both with pH = 1.4 ± 0.2 acid catholyte, and AEM with pH = 7.5 ± 0.1 catholyte (PBS buffer). The use of an acidic catholyte in the MEC with an AEM was not examined as sulfate ions can be transported into the anode chamber and combined with the protons from acetate oxidation, resulting in the acidification of the anolyte. Therefore, only a neutral pH catholyte was used for the AEM to compare to previous MEC studies with neutral pH conditions.

**Electrochemical Characterization.** The resistances and working potentials of the electrodes of the MECs were calculated using the EPS method.<sup>21,22</sup> This method allows the direct comparison of electrochemical performance of the MECs that have different configurations. Polarization data were collected at near maximum current density by varying the applied voltage from 1.0 to 0 V and measuring the current based on the voltage changes across a 10 Ω resistor at 20 min intervals. The polarization data were linearized using  $E = mj + b$ , where  $j$  is the current density, the absolute value of the slope  $m$  is the specific resistance of the anode ( $R_{An}$ ) or cathode ( $R_{Cat}$ ) (mΩ m<sup>2</sup>), and the  $y$ -intercepts of polarization curves are used as the experimental open circuit potentials of the anode ( $E_{An,oc}$ ) or cathode ( $E_{Cat,oc}$ ).<sup>21</sup> This method assumes that the system is operating under steady-state conditions over the

linearized current density range. The solution resistance for each electrolyte ( $R_{Ω,An}$  and  $R_{Ω,Cat}$ ) was calculated based on the solution conductivity ( $σ$ , mS/cm), the distance between the electrode and membrane ( $l$ , cm) and the cross-sectional area of the reactor ( $A$ , cm<sup>2</sup>) using  $R_{Ω,An} = R_{Ω,Cat} = 10^3 l / σ A$ .<sup>26</sup> The membrane ( $R_{Ω,mem}$ ) was calculated as the unknown based on the individual resistances and the total internal resistance of the cell ( $R_{cell}$ ) obtained using  $R_{cell} = R_{Cat} + R_{An} + R_{Ω,An} + R_{Ω,Cat} + R_{Ω,mem}$ .<sup>22</sup>

#### Analytical Methods and Performance Calculations.

The hydrogen and nitrogen gas compositions in the headspace and gas bag were analyzed using a gas chromatograph (model 310, SRI Instruments Inc., US). The volume of hydrogen gas was determined using the gas bag method as previously described.<sup>27</sup> For this method, gas in the gas bag was evacuated by vacuum and then the gas bag was connected to the MEC. At the end of the tests, gas in the headspace and the gas bag were analyzed, and then a known volume of N<sub>2</sub> gas was added (30 mL) into the bag and the gas re-analyzed to determine its H<sub>2</sub> volume by difference.

The hydrogen production rate was calculated by normalizing the volume of the hydrogen gas produced by the total solution volume (63 mL including the 28 mL of anolyte, 28 mL of catholyte and 7 mL headspace), and the elapsed time to complete 90% of the total transferred charge in order to avoid times at the end of cycles where there was little gas production.<sup>28</sup> The concentration of acetate consumed was calculated based on the initial and final chemical oxygen demands (CODs) measured using standard methods (method 5220, HACH). The solution pH and conductivity were monitored using a probe and meter (Seven-Multi, Mettler-Toledo International Inc., US).

The theoretical maximal production of hydrogen ( $n_{th}$ ) was calculated as

$$n_{th} = \frac{2\Delta COD}{M_{O_2}} \quad (1)$$

where  $M_{O_2}$  is the molecular weight of oxygen (32 g/mol) and  $\Delta COD$  is the difference between initial and final COD.<sup>19</sup> The moles of hydrogen that can be recovered based on the current produced,  $n_{CE}$ , is

$$n_{CE} = \frac{\int_{t=0}^t I dt}{2F} \quad (2)$$

where  $dt$  (s) is the interval over which 90% of the total coulombs are collected in terms of the current ( $I_{90}$ ), 2 is used to convert moles of electrons to moles of hydrogen, and  $F$  is the Faraday's constant. The Coulombic efficiency ( $C_E$ ) was calculated as  $C_E = n_{CE}/n_{th}$ , cathodic hydrogen recovery ( $r_{cat}$ ) calculated using  $r_{cat} = n_{H_2}/n_{CE}$ , and the overall hydrogen recovery ( $r_{H_2}$ ) as  $r_{H_2} = C_E r_{cat}$ .

The maximum energy recovery ( $\eta_E$ ) at neutral pH was calculated using<sup>19</sup>

$$\eta_E = 1.23 E_{ps}^{-1} \quad (3)$$

where  $E_{ps}$  is the applied voltage (V). This equation is modified using the Nernst equation to calculate the maximum energy recovery of MECs as a function of the anolyte or catholyte pH as



$$\eta_E = 1.23(E_{ps} - 0.059\Delta pH)^{-1} \quad (4)$$

## RESULTS AND DISCUSSION

**Impact of Catholyte pH on Maximum Current Densities.** The  $j_{\max}$  increased inversely with pH, with a maximum of  $10.6 \pm 0.3 \text{ A/m}^2$  obtained at a pH = 0.3 ( $226 \pm 6 \text{ mS/cm}$ ) using a 500 mM  $\text{H}_2\text{SO}_4$  catholyte (Figure 2). The  $j_{\max}$

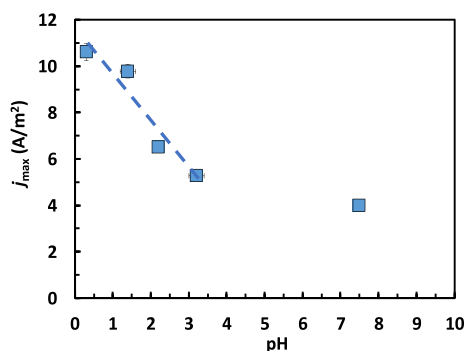


**Figure 2.** Impact of initial catholyte pH on the maximum current density of MEC using the BPM and Pt/C cathode.

decreased approximately linearly with pH over the range of 0.5–3.5, but then decreased less for the test at pH = 7.5, reflecting the importance of the proton concentration in the electrolyte and its limitation on HER at low concentrations (high pHs) (Figure 2). While the highest current density was obtained at a pH = 0.3, a high osmotic pressure difference across the membrane resulted in water migration ( $\sim 2 \text{ mL}$ ) from the anolyte into the catholyte (Figure S1). At other pHs there was a no detectable change in the anolyte volume occurred. Therefore, 50 mM  $\text{H}_2\text{SO}_4$  (pH =  $1.4 \pm 0.2$ ) was used in the catholyte in all subsequent tests to avoid water loss from the anolyte.

**Hydrogen Production and Performance.** The hydrogen production rate for the first cycle with the BPM membrane and Pt cathode was  $1.2 \pm 0.7 \text{ L-H}_2/\text{L/d}$  (pH = 1.4 catholyte). This rate was 2.8 times greater than that obtained with the same configuration using the AEM ( $0.43 \pm 0.1 \text{ L-H}_2/\text{L/d}$ ) (Figure 3a). Hydrogen production with the AEM here was similar to a previous report of using an AEM and neutral pH catholyte in the same type of MEC ( $0.38 \pm 0.02 \text{ L-H}_2/\text{L/d}$ ).<sup>29</sup> The maximum current of the BPM-Pt of  $j_{\max} = 10 \pm 0.4 \text{ A/m}^2$  was 1.5 times that of the AEM-Pt ( $j_{\max} = 6.5 \pm 0.3 \text{ A/m}^2$ ). There was little change in the catholyte pH over the cycle with the BPM-Pt (pH from  $1.4 \pm 0.2$  to  $1.6 \pm 0.2$ ), while the pH of the catholyte of the AEM-Pt increased to  $10 \pm 0.4$  from  $7.5 \pm 0.1$ .

As a result of the higher maximum current for the BPM-Pt configuration, the cycle time based on 90% of the transferred charge was  $21 \pm 1 \text{ h}$ , compared to about twice that for the AEM-Pt configuration ( $41 \pm 2 \text{ h}$ ) (Figure S2). Both systems had a final COD of  $\sim 90 \text{ mg/L}$ , but the Coulombic efficiency of the MECs using a BPM was  $90 \pm 5\%$ , compared to  $69 \pm 3\%$  for AEM-Pt (Figure 3b). The cathodic efficiency and overall hydrogen recovery for BPM-based reactors were slightly above 100%, likely due to small errors in the experimental measurement made using gas chromatography and the calculation of total charge transfer based on the integration of current output with time as the current was not measured continuously (in 20 min intervals). The maximum energy

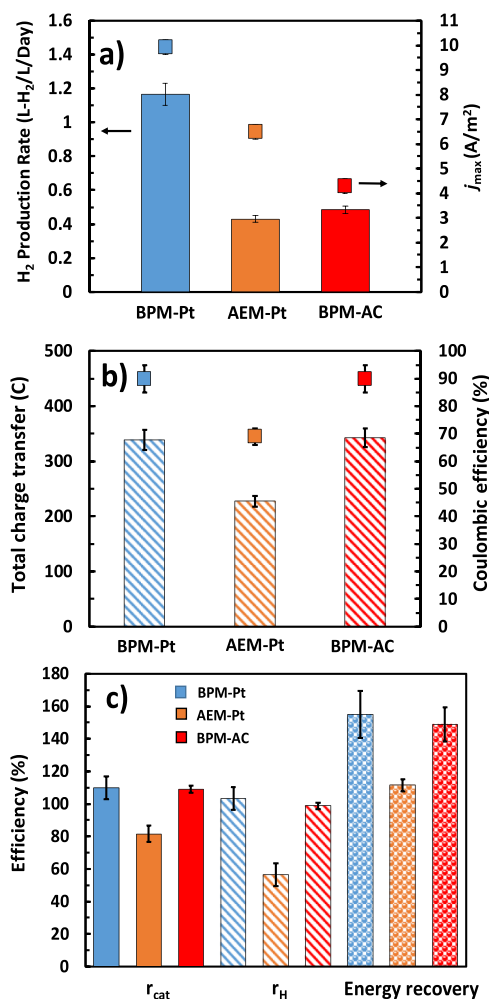


**Figure 3.** (a)  $\text{H}_2$  production rate ( $I_{90}$ ) and maximum current density, (b) total charge transfer and Coulombic efficiency, and (c)  $r_{\text{cat}}$ ,  $r_{\text{H}}$ , and energy yield of different MECs.

recovery was  $111 \pm 4\%$  for the AEM-Pt cell, compared to theoretical efficiencies of 137% based on the experimental conditions and the applied voltage (equation 3). The energy recovery was  $155 \pm 14\%$  for the BPM-Pt cell, compared to a calculated maximum energy recovery of 214% based on calculations that include the pH difference between the anolyte and catholyte using eq 4.

When the Pt catalyst was replaced with AC, the hydrogen production rate decreased to  $0.45 \pm 0.1 \text{ L-H}_2/\text{L/d}$  (BPM-AC), with a maximum current density of  $j_{\max} = 4.3 \pm 0.7 \text{ A/m}^2$  (Figure 3a). The hydrogen production rate was slightly higher than that of the MEC using an AEM and a Pt catalyst on the cathode. Coulombic efficiencies, cathodic recoveries, and energy recoveries for the BPM-AC configuration were all similar to that of the BPM-Pt cell and better than those for the AEM-Pt cell (Figure 3a,b), indicating that the improved performance based on these metrics was due to the use of the BPM and 50 mM  $\text{H}_2\text{SO}_4$ . The BPM with four layers of GO-BPM was also investigated as a method to improve performance. However, the MEC performance with the GO-BPM was the same as that using a commercial BPM (Figure S3). This was likely due to the applied voltage ( $\leq 1.0 \text{ V}$ ) being too low for effective catalysis for water dissociation.<sup>17</sup>

**Area-Specific Resistances.** The experimental maximum working circuit voltage, obtained from the difference of the y-

intercepts of the polarization curves of whole cells, was  $-0.15 \pm 0.01$  V for the BPM-Pt configuration (Figure 4a). Based on

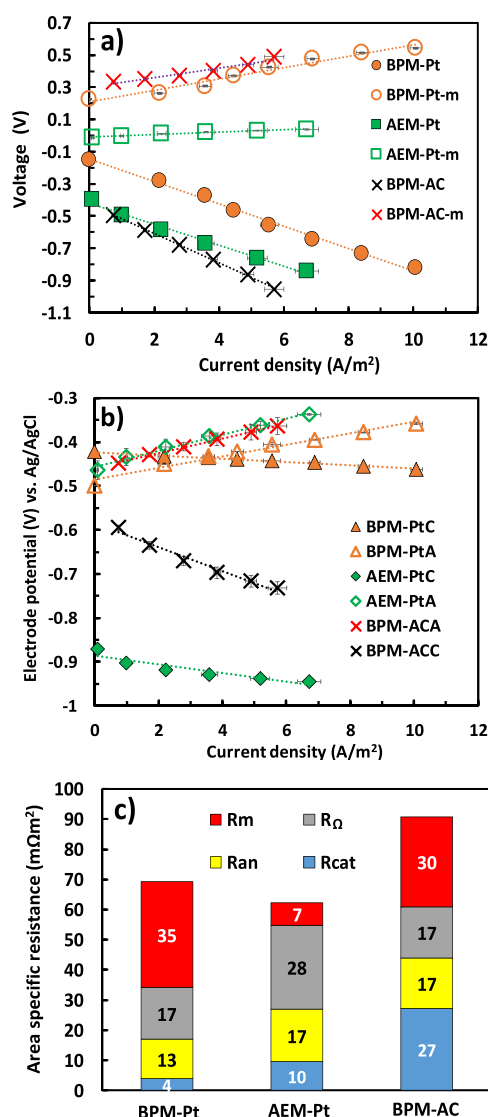


**Figure 4.** (a) Whole cell polarization curves and voltage losses for the different membranes (indicated by the letter m); and (b) polarization curves of the anodes and cathode for the BPM-Pt, AEM-Pt, and BPM-AC MECs (indicated with A = anode, and C = cathode) with an applied voltage of 0.9 V. (c) Area-specific resistances of MEC components ( $R_m$  = membrane,  $R_{An}$  = anode,  $R_{Cat}$  = cathode, and  $R_{\Omega}$  = solution).

the pH difference between the anolyte and the catholyte ( $7.5 - 1.4 = 6.1$ ), the potential difference between two chambers in the BPM-Pt cells using Nernst equation was  $6.1 \times 0.059 = 0.36$  V, which is used for compensating the voltage drop over the BPM for water dissociation. The whole cell voltages for the other two configurations were more negative by  $\sim 0.25$  V compared to the BPM-Pt cell but they were similar to each other ( $-0.43 \pm 0.01$  V for AEM-Pt, and  $-0.42 \pm 0.02$  V for BPM-AC). This more negative voltage for the BPM-AC configuration was consistent with the AC being a poor catalyst for the HER.

The voltage losses across the membranes in the MECs were calculated from the whole cell voltages and the other component resistances. The voltage loss for the BPM with

the Pt cathode, based on the intercepts (zero current), was  $0.21 \pm 0.02$  V, which was only slightly higher than that of the BPM with the AC cathode ( $0.28 \pm 0.03$  V) (Figure 4a). Theoretically, these two voltages should be the same, but differences arise from the combined errors in other experimental measurements. The AEM had a calculated open circuit voltage of  $\sim 0$  V, demonstrating little voltage loss for this membrane.

The cathode potential for the BPM-Pt configuration was more positive than the anode potential at applied voltages of  $< 0.4$  V (Figure 4b). The measured cathode potential of the BPM-Pt cell at zero current was  $-0.43 \pm 0.01$  V, compared to  $-0.88 \pm 0.02$  V for the AEM-Pt. In theory, the calculated potential difference based on the pH difference between two cathodes could reach 0.36 V. The larger difference of the measured cathode potentials ( $0.88 - 0.43$  V = 0.45 V) reflects the increased catholyte pHs for the AEM-Pt, which would shift its HER potential to more negative values. The anode potentials using the BPM-Pt were more negative using the other two cases (Figure 4b), perhaps because of slightly better acclimated anodes for the higher current densities.

The area-specific resistances of each of the components of the MECs can be used to examine the tradeoffs in the different operational conditions. The BPM-Pt MECs had a lower total internal resistance at an applied voltage of 0.9 V of  $70 \pm 2$  mΩ m<sup>2</sup>, compared to that of the BPM-AC MEC ( $90 \pm 3$  mΩ m<sup>2</sup>), primarily due to the much lower cathode resistance using Pt instead of AC for the catalyst (Figure 4c). The AEM-Pt configuration had the lowest total area resistance of  $65 \pm 3$  mΩ m<sup>2</sup> because of the low AEM resistance ( $7.5 \pm 0.4$  mΩ m<sup>2</sup>) compared to much higher resistances for the BPMs. This AEM resistance compares well to that previously found for this MEC ( $6 \pm 5$  mΩ m<sup>2</sup>).<sup>22</sup> The membrane was the biggest contributor to the area-specific resistance of BPM-MECs, with  $35 \pm 2$  mΩ m<sup>2</sup> for the BPM-Pt and  $30 \pm 1.5$  mΩ m<sup>2</sup> for the BPM-AC. The resistance of the catholyte was only marginally reduced by employing an acidic solution ( $4 \pm 0.3$  mΩ m<sup>2</sup>) for the Pt catalyst with the BPM, compared to  $10 \pm 1$  mΩ m<sup>2</sup> for the neutral pH catholyte with the AEM (Figure 4c). Thus, the greater impact of the acid catholyte was to produce more positive potentials of the cathode in the acidic as shown above. The area-specific resistance of bio-anodes in all MECs was consistent with the values reported previously.<sup>21,22</sup>

**Stability over Multiple Cycles.** When the performance of the system was examined over multiple cycles, the maximum current density of the BPM-Pt based cell decreased with each cycle, with  $j_{max} = 11 \pm 0.6$  A/m<sup>2</sup> in the first cycle,  $4.1 \pm 0.2$  A/m<sup>2</sup> after 6 days (Figure 5a). This decrease in performance was clearly due to the cathode potential becoming more negative, indicating a less thermodynamically favorable HER (Figure 5b). Although the current density of the BPM-AC MEC was much lower, the performance was more stable over each daily cycle, decreasing from a maximum current density of  $4.2 \pm 0.2$  A/m<sup>2</sup> on the first cycle, to  $3.4 \pm 0.1$  after 12 days along with a reduction in the cathode potential (Figure 5c,d). In abiotic electrolysis cells, as the current increases by using higher applied voltages ( $> 1.5$  V) co-ion leakage will be reduced, and thus the pH stability of the catholyte improved. However, water dissociation is not as effective at lower applied voltages (e.g., 0.9 V in our study). If the HER has a high rate due to the use of a good catalyst (e.g., Pt/C), the protons in the cathode solution will be consumed rapidly, resulting in a larger change of catholyte pH. For example, the pH of the BPM-Pt cell

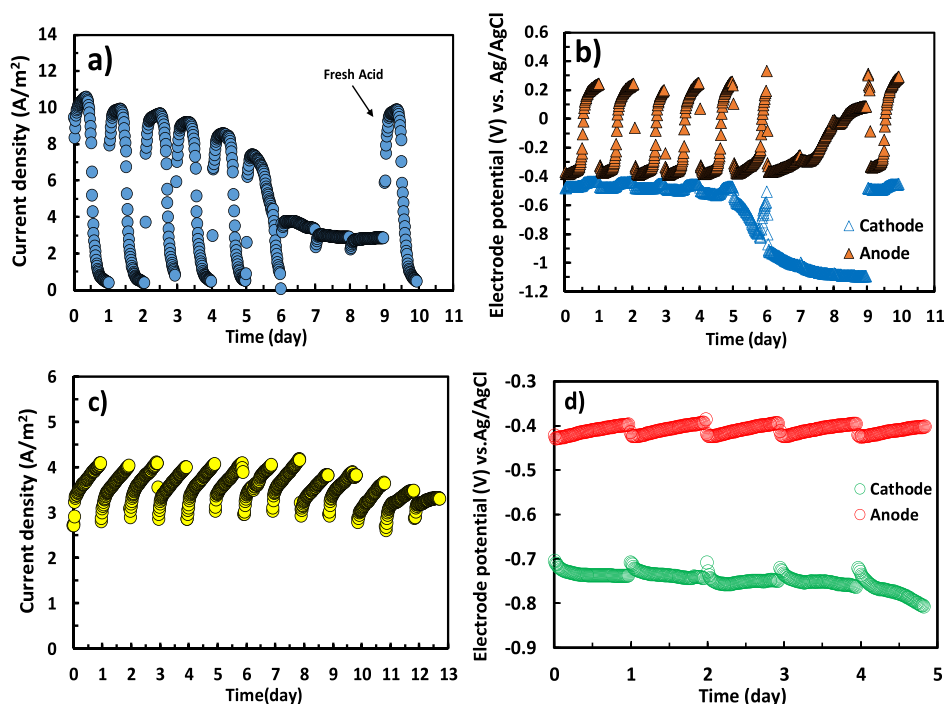


**Figure 5.** Performance stability of BPM-MECs (a) BPM-Pt cell, (b) electrode potential of BPM-Pt, (c) BPM-AC cell, and (d) electrode potential of BPM-AC during the last 5 days.

catholyte was constantly increasing during operation, and the conductivity was decreasing, from  $\text{pH} = 1.4 \pm 0.2$  and  $\sigma = 25 \pm 0.5 \text{ mS/cm}$  on the first day, to a  $\text{pH} = 11 \pm 0.3$  and  $\sigma = 8.2 \pm 0.5 \text{ mS/cm}$  after 9 days. However, while a decay in performance was observed with the BPM-AC configuration, the rate was much slower, and therefore the final catholyte pH in the BPM-AC reactor was much lower ( $\text{pH} = 2.5 \pm 0.2$ ,  $\sigma = 11.6 \pm 0.3 \text{ mS/cm}$ ) than that of BPM-Pt reactor. Both reactors resumed performance to the original levels when the catholyte was replaced with fresh solutions (data not shown for the BPM-AC cell). The results demonstrated that despite the use of the BPM and AC cathode, a change in the catholyte pH could be delayed but not prevented. Thus, there was likely leakage of ions across the BPM in addition to water dissociation.

**Comparison of the Two BPM MECs at Similar Current Densities.** To further examine the relative importance of an ion crossover compared to water dissociation, the BPM-Pt MEC was operated at a lower applied voltage of 0.46 V to produce a current density more similar to that of the BPM-AC reactor (Figure 6). In these tests, each cycle lasted for 2 days. At 0.46 V, the BPM-Pt configuration produced a maximum current density of  $j_{\text{max}} = 3.5 \pm 0.3 \text{ A/m}^2$  (after adjusting the applied voltage to 0.46 V), with a total charge transferred being  $1735 \pm 65 \text{ C}$  over the 5 cycles (10 days), compared to  $j_{\text{max}} = 4.0 \pm 0.1 \text{ A/m}^2$  and  $2097 \pm 30 \text{ C}$  for the BPM-AC at 0.9 V applied voltage. After 10 days, the final catholyte pH of BPM-Pt ( $4.7 \pm 0.3$ ) was higher than that of BPM-AC MEC ( $2.2 \pm 0.2$ ). The observation that more charge was transferred (more protons were consumed) using the BPM-AC, but the final catholyte pH was lower, suggesting that more protons were generated from the BPM with an AC cathode under the higher applied voltage.

**Overall Analysis.** Using a BPM in an MEC with an acidic catholyte and Pt cathode catalyst was effective for increasing

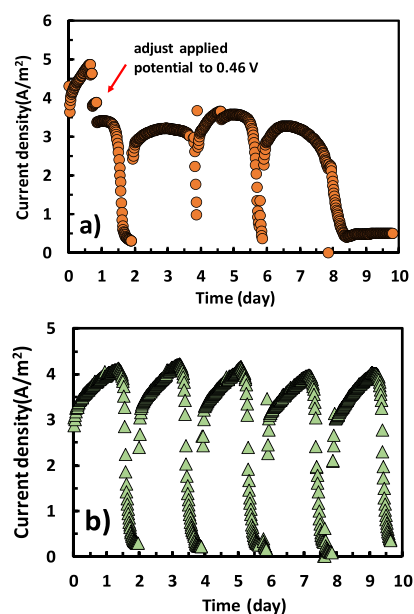


**Figure 6.** Performance stability of BPM MECs at different applied potentials (a) 0.46 V for the BPM-Pt MEC and (b) 0.9 V for the BPM-AC MEC. The initial catholyte conditions were  $\text{pH} = 1.4 \pm 0.2$  and  $\sigma = 25 \pm 0.5 \text{ mS/cm}$ .

the current density compared to an MEC with an AEM and neutral pH catholyte. While the MEC with the AEM reached a highly alkaline pH after each cycle, and the catholyte had to be replaced after each cycle, the MEC with the BPM was able to operate for 9 cycles before the pH become highly alkaline because of the faster consumption of protons using the Pt/C cathode. The observation that the catholyte pH did slowly increase under low current densities using AC cathodes showed that the BPM did not operate only under water



dissociation conditions, and charge leakage of other ions occurred across the membrane. However, it is known that BPMs cannot perfectly maintain charge balances and that charge leakage is a function of both current density and pH differences between adjacent electrolyte chambers.<sup>14</sup>

The performance of the MECs without a precious metal catalyst, for example, using AC alone or with the addition of the Ni catalyst, has economic benefits.<sup>8</sup> The nonmetal AC catalyst is only \$2.6/kg compared to Pt/C (\$140/g) which is a much less abundant precious metal, and the use of Pt would be too expensive and not abundant to make its use economical in an MEC for wastewater treatment.<sup>30</sup> The cost of the BPM from different manufactures is variable and can be as low as \$700 per square meter for small orders (Yichen Technology, China), but it could be significantly reduced in cost to ~\$100 by purchasing large quantities. Thus, although the current densities and hydrogen production rates were lower with the BPM-AC MEC, compared to that with a Pt cathode, the hydrogen production rate was similar to or better than that of the MEC with the AEM and Pt catalyst.

The use of an acidic catholyte has other advantages for operation of MECs, for example, suppressing the growth of methanogens and other microorganisms that might oxidize the hydrogen, and the acidic pH that reduces cross-over of most chemical species (except protons). There is an additional cost, however, of maintaining an acidic catholyte that would need to be balanced against the value of the hydrogen gas that was produced in the process, and potential benefits for treating a wastewater in the anolyte.

## ■ ASSOCIATED CONTENT

### Supporting Information

The Supporting Information is available free of charge at <https://pubs.acs.org/doi/10.1021/acs.est.9b05024>.

Height change of 0.5 M H<sub>2</sub>SO<sub>4</sub> catholyte, current density output of different MECs, and polarization curves of BPM-Pt and GOBPM-Pt (PDF)

## ■ AUTHOR INFORMATION

### Corresponding Authors

\*E-mail: [xu.wang@whu.edu.cn](mailto:xu.wang@whu.edu.cn). Phone: +86-159-272-98667 (X.W.).

\*E-mail: [blogan@psu.edu](mailto:blogan@psu.edu). Phone: +1-814-863-7908. Fax: +1 814 863-7304 (B.E.L.).

### ORCID

Bruce E. Logan: 0000-0001-7478-8070

### Notes

The authors declare no competing financial interest.

## ■ ACKNOWLEDGMENTS

This research was supported by the China Scholarship Council (no. 201706275155), Penn State University, the National Major Project of Water Pollution Control and Treatment (no. 2017ZX07204004-01), and the Fundamental Research Funds for the Central Universities (grant no. 2042018kf0244). Work on the synthesis and characterization of BPMs by Z.Y. and T.E.M. was supported by the Office of Basic Energy Sciences, Division of Chemical Sciences, Geosciences, and Energy Biosciences, Department of Energy, under contract DE-FG02-07ER15911.

## ■ REFERENCES

- (1) Logan, B. E.; Rabaey, K. Conversion of wastes into bioelectricity and chemicals by using microbial electrochemical technologies. *Science* **2012**, *337*, 686–690.
- (2) Cheng, S.; Logan, B. E. Sustainable and efficient biohydrogen production via electrohydrogenesis. *Proc. Natl. Acad. Sci. U.S.A.* **2007**, *104*, 18871.
- (3) Lu, L.; Ren, Z. J. Microbial electrolysis cells for waste biorefinery: A state of the art review. *Bioresour. Technol.* **2016**, *215*, 254–264.
- (4) Cusick, R. D.; Bryan, B.; Parker, D. S.; Merrill, M. D.; Mehanna, M.; Kiely, P. D.; Liu, G.; Logan, B. E. Performance of a pilot-scale continuous flow microbial electrolysis cell fed winery wastewater. *Appl. Microbiol. Biotechnol.* **2011**, *89*, 2053–2063.
- (5) Montpart, N.; Rago, L.; Baeza, J. A.; Guisasola, A. Hydrogen production in single chamber microbial electrolysis cells with different complex substrates. *Water Res.* **2015**, *68*, 601–615.
- (6) Baeza, J. A.; Martínez-Miró, À.; Guerrero, J.; Ruiz, Y.; Guisasola, A. Bioelectrochemical hydrogen production from urban wastewater on a pilot scale. *J. Power Sources* **2017**, *356*, 500–509.
- (7) Rozendal, R. A.; Hamelers, H. V. M.; Molenkamp, R. J.; Buisman, C. J. N. Performance of single chamber biocatalyzed electrolysis with different types of ion exchange membranes. *Water Res.* **2007**, *41*, 1984–1994.
- (8) Kim, K.-Y.; Yang, W.; Logan, B. E. Regenerable nickel-functionalized activated carbon cathodes enhanced by metal adsorption to improve hydrogen production in microbial electrolysis cells. *Environ. Sci. Technol.* **2018**, *52*, 7131–7137.
- (9) Jeremiasse, A. W.; Hamelers, H. V. M.; Saakes, M.; Buisman, C. J. N. Ni foam cathode enables high volumetric H<sub>2</sub> production in a microbial electrolysis cell. *Int. J. Hydrogen Energy* **2010**, *35*, 12716–12723.
- (10) Sleutels, T. H. J. A.; Hamelers, H. V. M.; Rozendal, R. A.; Buisman, C. J. N. Ion transport resistance in Microbial Electrolysis Cells with anion and cation exchange membranes. *Int. J. Hydrogen Energy* **2009**, *34*, 3612–3620.
- (11) Sleutels, T. H. J. A. Membrane Selectivity Determines Energetic Losses for Ion Transport in Bioelectrochemical Systems. *ChemistrySelect* **2017**, *2*, 3462–3470.
- (12) Ruiz, Y.; Baeza, J. A.; Guisasola, A. Microbial electrolysis cell performance using non-buffered and low conductivity wastewaters. *Chem. Eng. J.* **2016**, *289*, 341–348.
- (13) Sun, K.; Liu, R.; Chen, Y.; Verlage, E.; Lewis, N. S.; Xiang, C. A stabilized, intrinsically safe, 10% efficient, solar driven water splitting cell incorporating earth abundant electrocatalysts with steady-state pH gradients and product separation enabled by a bipolar membrane. *Adv. Energy Mater.* **2016**, *6*, 1600379.
- (14) Vermaas, D. A.; Wiegman, S.; Nagaki, T.; Smith, W. A. Ion transport mechanisms in bipolar membranes for (photo)-electrochemical water splitting. *Sustainable Energy Fuels* **2018**, *2*, 2006–2015.
- (15) Harnisch, F.; Schröder, U.; Scholz, F. The suitability of monopolar and bipolar ion exchange membranes as separators for biological fuel cells. *Environ. Sci. Technol.* **2008**, *42*, 1740–1746.
- (16) Vargas-Barbosa, N. M.; Geise, G. M.; Hickner, M. A.; Mallouk, T. E. Assessing the utility of bipolar membranes for use in photoelectrochemical water-splitting cells. *ChemSusChem* **2014**, *7*, 3017–3020.
- (17) Yan, Z.; Zhu, L.; Li, Y. C.; Wycisk, R. J.; Pintauro, P. N.; Hickner, M. A.; Mallouk, T. E. The balance of electric field and interfacial catalysis in promoting water dissociation in bipolar membranes. *Energy Environ. Sci.* **2018**, *11*, 2235–2245.
- (18) Vermaas, D. A.; Sassenburg, M.; Smith, W. A. Photo-assisted water splitting with bipolar membrane induced pH gradients for practical solar fuel devices. *J. Mater. Chem. A* **2015**, *3*, 19556–19562.
- (19) Logan, B. E.; Call, D.; Cheng, S.; Hamelers, H. V. M.; Sleutels, T. H. J. A.; Jeremiasse, A. W.; Rozendal, R. A. Microbial electrolysis cells for high yield hydrogen gas production from organic matter. *Environ. Sci. Technol.* **2008**, *42*, 8630–8640.

- (20) Lu, L.; Vakki, W.; Aguiar, J. A.; Xiao, C.; Hurst, K.; Fairchild, M.; Chen, X.; Yang, F.; Gu, J.; Ren, Z. J. Unbiased solar H<sub>2</sub> production with current density up to 23 mA cm<sup>-2</sup> by Swiss-cheese black Si coupled with wastewater bioanode. *Energy Environ. Sci.* **2019**, *12*, 1088–1099.
- (21) Rossi, R.; Cario, B. P.; Santoro, C.; Yang, W.; Saikaly, P. E.; Logan, B. E. Evaluation of electrode and solution area-based resistances enables quantitative comparisons of factors impacting microbial fuel cell performance. *Environ. Sci. Technol.* **2019**, *53*, 3977–3986.
- (22) Cario, B. P.; Rossi, R.; Kim, K.-Y.; Logan, B. E. Applying the electrode potential slope method as a tool to quantitatively evaluate the performance of individual microbial electrolysis cell components. *Bioresour. Technol.* **2019**, *287*, 121418.
- (23) Ribot-Llobet, E.; Nam, J.-Y.; Tokash, J. C.; Guisasola, A.; Logan, B. E. Assessment of four different cathode materials at different initial pHs using unbuffered catholytes in microbial electrolysis cells. *Int. J. Hydrogen Energy* **2013**, *38*, 2951–2956.
- (24) Yang, W.; Logan, B. E. Immobilization of a Metal–Nitrogen–Carbon Catalyst on Activated Carbon with Enhanced Cathode Performance in Microbial Fuel Cells. *ChemSusChem* **2016**, *9*, 2226–2232.
- (25) Kovtyukhova, N. I.; Ollivier, P. J.; Martin, B. R.; Mallouk, T. E.; Chizhik, S. A.; Buzaneva, E. V.; Gorchinskiy, A. D. Layer-by-layer assembly of ultrathin composite films from micron-sized graphite oxide sheets and polycations. *Chem. Mater.* **1999**, *11*, 771–778.
- (26) Logan, B. E.; Zikmund, E.; Yang, W.; Rossi, R.; Kim, K.-Y.; Saikaly, P. E.; Zhang, F. Impact of ohmic resistance on measured electrode potentials and maximum power production in microbial fuel cells. *Environ. Sci. Technol.* **2018**, *52*, 8977–8985.
- (27) Ambler, J. R.; Logan, B. E. Evaluation of stainless steel cathodes and a bicarbonate buffer for hydrogen production in microbial electrolysis cells using a new method for measuring gas production. *Int. J. Hydrogen Energy* **2011**, *36*, 160–166.
- (28) Ivanov, I.; Ren, L.; Siegert, M.; Logan, B. E. A quantitative method to evaluate microbial electrolysis cell effectiveness for energy recovery and wastewater treatment. *Int. J. Hydrogen Energy* **2013**, *38*, 13135–13142.
- (29) Zikmund, E.; Kim, K.-Y.; Logan, B. E. Hydrogen production rates with closely-spaced felt anodes and cathodes compared to brush anodes in two-chamber microbial electrolysis cells. *Int. J. Hydrogen Energy* **2018**, *43*, 9599–9606.
- (30) Zhang, F.; Cheng, S.; Pant, D.; Bogaert, G. V.; Logan, B. E. Power generation using an activated carbon and metal mesh cathode in a microbial fuel cell. *Electrochem. Commun.* **2009**, *11*, 2177–2179.